

Spectroscopic detection of CIV λ 1548 in a galaxy at $z = 7.045$: Implications for the ionizing spectra of reionization-era galaxies

Daniel P. Stark^{1*}, Gregory Walth¹, Stéphane Charlot², Benjamin Clément³, Anna Feltre², Julia Gutkin², Johan Richard³, Ramesh Mainali¹, Brant Robertson¹, Brian Siana⁴, Mengtao Tang¹ & Matthew Schenker⁵

¹ Steward Observatory, University of Arizona, 933 N Cherry Ave, Tucson, AZ 85721 USA

² Sorbonne Universités, UPMC-CNRS, UMR7095, Institut d’Astrophysique de Paris, F-75014 Paris, France

³ Centre de Recherche Astrophysique de Lyon, Université Lyon 1, 9 Avenue Charles Andre, 69561, France

⁴ Department of Physics & Astronomy, University of California, Riverside, CA 92507 USA

⁵ PDT Partners, LLC, 1745 Broadway, NY, NY 10019 USA

28 April 2015

ABSTRACT

We present Keck/MOSFIRE observations of UV metal lines in four bright ($H=23.9-25.4$) gravitationally-lensed $z \simeq 6 - 8$ galaxies behind the cluster Abell 1703. The spectrum of A1703-zd6, a highly-magnified star forming galaxy with a Ly α redshift of $z = 7.045$, reveals a confident ($S/N=5.1$) detection of the nebular CIV λ 1548 emission line (unresolved with $\text{FWHM} < 125 \text{ km s}^{-1}$). UV metal lines are not detected in the three other galaxies. At $z \simeq 2 - 3$, nebular CIV emission is observed in just 1% of UV-selected galaxies. The presence of strong CIV emission in one of the small sample of galaxies targeted in this paper may indicate hard ionizing spectra are more common at $z \simeq 7$. The total estimated equivalent width of the CIV doublet ($W_{\text{CIV}} \simeq 38 \text{ \AA}$) and CIV/Ly α flux ratio ($f_{\text{CIV}}/f_{\text{Ly}\alpha} \simeq 0.3$) are comparable to measurements of narrow-lined AGNs. Photoionization models show that the nebular CIV line can also be reproduced by a young stellar population, with very hot metal poor stars dominating the photon flux responsible for triply ionizing carbon. Regardless of the origin of the CIV, we show that the ionizing spectrum of A1703-zd6 is different from that of typical galaxies at $z \simeq 2$, producing more H ionizing photons per unit 1500 \AA luminosity ($\log(\xi_{\text{ion}}/\text{erg}^{-1} \text{ Hz})=25.68$) and a larger flux density at 30-50 eV. If such extreme radiation fields are typical in UV-selected systems at $z \gtrsim 7$, it would indicate that reionization-era galaxies are more efficient ionizing agents than previously thought. Alternatively, we suggest that the small sample of Ly α emitters at $z \gtrsim 7$ may trace a rare population with intense radiation fields capable of ionizing their surrounding hydrogen distribution. Additional constraints on high ionization emission lines in galaxies with and without Ly α detections will help clarify whether hard ionizing spectra are common in the reionization era.

Key words: cosmology: observations - galaxies: evolution - galaxies: formation - galaxies: high-redshift

1 INTRODUCTION

Our understanding of galaxy growth in the first billion years of cosmic time has developed rapidly in the last five years following a series of deep imaging campaigns with the infrared channel of the Wide Field Camera 3 (WFC3/IR) onboard the *Hubble Space Telescope* (HST). Deep WFC3/IR exposures have delivered more than

~ 1500 galaxies photometrically-selected to lie between $\simeq 0.5 - 1$ Gyr after the Big Bang (e.g. Bouwens et al. 2014b) and the first small samples of galaxies within the first 0.5 Gyr of cosmic time (e.g., Zheng et al. 2012; Ellis et al. 2013; Coe et al. 2013; Atek et al. 2015; Zitrin et al. 2014; Oesch et al. 2014).

These studies demonstrate that the $z \gtrsim 6$ galaxy population is different from well-studied samples at $z \simeq 2 - 3$. The UV luminosities, star formation rates, and stellar masses tend to be lower at $z \simeq 6$ (e.g. Smit et al. 2012; McLure et al. 2013; Schenker et al. 2013b; Bouwens et al. 2014a; Salmon et al. 2015; Duncan et al.

* dpstark@email.arizona.edu

2014; Grazian et al. 2015), the sizes are smaller (e.g., Oesch et al. 2010; Ono et al. 2013; c.f., Curtis-Lake et al. 2014), and the UV continuum colors are bluer (e.g., Wilkins et al. 2011; Finkelstein et al. 2012; Rogers et al. 2013; Bouwens et al. 2014a). Specific star formation rates at $z \gtrsim 6$ are large, indicating a rapidly growing young stellar population (e.g., Stark et al. 2013; González et al. 2014; Salmon et al. 2015).

The emission line properties of early galaxies also appear different. Large equivalent width Ly α emission is more common among $z \simeq 6$ galaxies than it is in similar systems at $z \simeq 3$ (e.g., Stark et al. 2011; Curtis-Lake et al. 2012). The strongest rest-frame optical lines ([OIII], H α) are more difficult to characterize since they are situated at $3 - 5\mu\text{m}$, where thermal emission from the atmosphere impedes detection with ground-based facilities. Nevertheless progress has been achieved by isolating galaxies at redshifts in which the [OIII] or H α line contaminates the Spitzer/IRAC broadband filters. In the last several years, this technique has been used to characterize the equivalent width distribution of H α in $3.8 < z < 5.0$ galaxies (Shim et al. 2011; Stark et al. 2013) and [OIII]+H β in $z \simeq 6.6 - 6.9$ (Smit et al. 2014, 2015) and $z \simeq 8$ (Labbé et al. 2013) galaxies, revealing that typical [OIII] and H α equivalent widths of $z \simeq 4 - 7$ galaxies are significantly larger than among similar systems at $z \simeq 2$. The population of extreme emission line galaxies (EW = 500-1000 Å), relatively rare among $z \simeq 1 - 2$ galaxies (e.g., Atek et al. 2011, van der Wel et al. 2011), appears to be ubiquitous at $z \simeq 7$ (Smit et al. 2014, 2015).

The common presence of extreme optical line emission holds clues as to the physical nature of $z \gtrsim 7$ galaxies. Recent work has demonstrated that optical line ratios among $z \simeq 2$ galaxies require an ionizing radiation field that is harder than in $z \simeq 0$ galaxies (e.g., Steidel et al. 2014), consistent with a blackbody with mean effective temperatures of 50,000-60,000 K. The increased incidence of extreme line emitters at $z \simeq 7$ with respect to $z \simeq 2$ may suggest that the net ionizing field is powered by even hotter stars at $z \simeq 7$. Such a finding would indicate that galaxies are very efficient ionizing agents throughout the tail end of the reionization era and would have important implications for the nature of the massive stars within $z \simeq 7$ galaxies.

Further progress in our understanding of the radiation field of early galaxies will only come from detailed spectroscopy. Prior to JWST, spectroscopic observations of $z \gtrsim 7$ galaxies will be limited to the rest-frame far-ultraviolet (FUV) window. The FUV contains several emission lines with higher ionization potential than in the rest-frame optical (i.e., CIV, He II), providing a valuable probe of the ionizing spectrum. While nebular emission from these species is rarely seen among luminous star forming galaxies, they have been identified more commonly in metal poor galaxies with low masses (Erb et al. 2010; Christensen et al. 2012; Stark et al. 2014b). Such systems also commonly show strong emission from the OIII] $\lambda\lambda 1660, 1666$ and CIII] $\lambda\lambda 1907, 1909$ intercombination lines (Garnett et al. 1995, 1997, 1999; Erb et al. 2010; Bayliss et al. 2014; James et al. 2014; Stark et al. 2014b).

Little is currently known about whether FUV spectra of galaxies in the reionization era. But with the discovery of an increasing number of bright $z \gtrsim 6$ galaxies (e.g., Bradley et al. 2014; Bowler et al. 2014), this is now beginning to change. Recently Stark et al. (2014a) reported tentative CIII] detections in two galaxies with previously confirmed redshifts ($z = 6.029$ and $z = 7.213$) from Ly α . Here we build on this progress with an exploration of the strength of high ionization emission features (CIV $\lambda\lambda 1548, 1551$ and He II $\lambda 1640$) in a small sample of $z \simeq 7$ UV-selected galaxies using the MOSFIRE (McLean et al. 2012) spectrograph on the Keck I tele-

Source	z_{spec}	z_{phot}	H ₁₆₀	UV lines targeted	Ref
A1703-zd1a	...	6.6-6.9	23.9	CIV, He II, OIII]	[1]
A1703-zd4	...	7.0-9.3	25.4	Ly α , CIV [†]	[1]
A1703-zd6	7.043	...	25.9	CIV, He II, OIII]	[1]
A1703-23	5.828	...	23.8	CIII]	[2]

Table 1. High redshift galaxies targeted with our Keck/MOSFIRE observations. Details on observations and reduction are presented in §2. The final column provides the reference to the article where the galaxy was first discussed in the literature. The magnitude of A1703-23 is from the H-band filter on Subaru/MOIRCS, while the others are from WFC3/IR imaging in the H₁₆₀ filter. For A1703-zd4, the † symbol marks the fact that we are sensitive to CIV over only a portion of the redshift range suggested by the photometry. References: [1] Bradley et al. (2012); [2] Richard et al. (2009).

scope. We report the detection of strong nebular CIV $\lambda 1548$ emission in the spectrum of A1703-zd6, a spectroscopically confirmed galaxy at $z = 7.045$. The total CIV equivalent width is greater than in existing samples of $z \simeq 2$ metal poor star forming galaxies (Christensen et al. 2012; Stark et al. 2014b) but is similar to that seen in narrow-lined AGNs (Hainline et al. 2011; Alexandroff et al. 2013), pointing to a hard radiation field in one of the most distant known galaxies.

Other galaxies on the MOSFIRE mask include a spectroscopically confirmed Ly α emitting galaxy at $z = 5.828$ (Richard et al. 2009) and A1703-zd1a, a photometrically-selected galaxy thought to lie in the range $z \simeq 6.6 - 6.9$ with *Spitzer*/IRAC colours (Bradley et al. 2012; Smit et al. 2014) indicating extreme [OIII]+H β emission in the rest-frame optical, and a bright z -band dropout (A1703-zd4 in Bradley et al. (2012)) with photometry suggesting a redshift in the range $z = 7.0 - 9.3$. No strong emission lines are seen in any of these systems.

The plan of the paper is as follows. In §2 we describe the MOSFIRE observations. The spectra are discussed in §3, and the photoionization modelling procedure is described in §4. We explore implications of our findings in §5 and summarize the results in §6. We adopt a Λ -dominated, flat Universe with $\Omega_{\Lambda} = 0.7$, $\Omega_M = 0.3$ and $H_0 = 70 h_{70} \text{ km s}^{-1} \text{ Mpc}^{-1}$. All magnitudes in this paper are quoted in the AB system (Oke & Gunn 1983).

2 KECK/MOSFIRE OBSERVATIONS

Near-infrared spectroscopic observations of Abell 1703 were carried out with MOSFIRE (McLean et al. 2010, 2012) on the Keck-I Telescope on April 11, 2014 UT. The spectroscopic observations were taken using the YJ grating with the J-band filter, which has a resolution of $R=3318$ and covers a wavelength range of $\lambda=1.15-1.35\mu\text{m}$. A mask was created for Abell 1703 with $1''.0$ width slits. Individual exposures were 120 seconds with two position dithers of $3''.0$ having a total integration time of 2.6 hours. The average seeing throughout the observation was $0''.80$ (FWHM).

The spectra were reduced using the MOSFIRE Data Reduction Pipeline (DRP). The MOSFIRE DRP performs the standard NIR spectroscopic reduction; flat-fielding, wavelength calibration, sky-subtraction, and Cosmic Ray removal to produce 2D spectra. The flux calibration was performed using a star placed in the mask of the science field with HST ACS/WFC3 photometry. The flux from the star was scaled by the HST photometry and the spectral slope was corrected by fitting a power law between photometric bands. The 1D-spectra were extracted with $1''.1$, $1''.4$ and $1''.8$ (6, 8, 10 pixels) apertures.

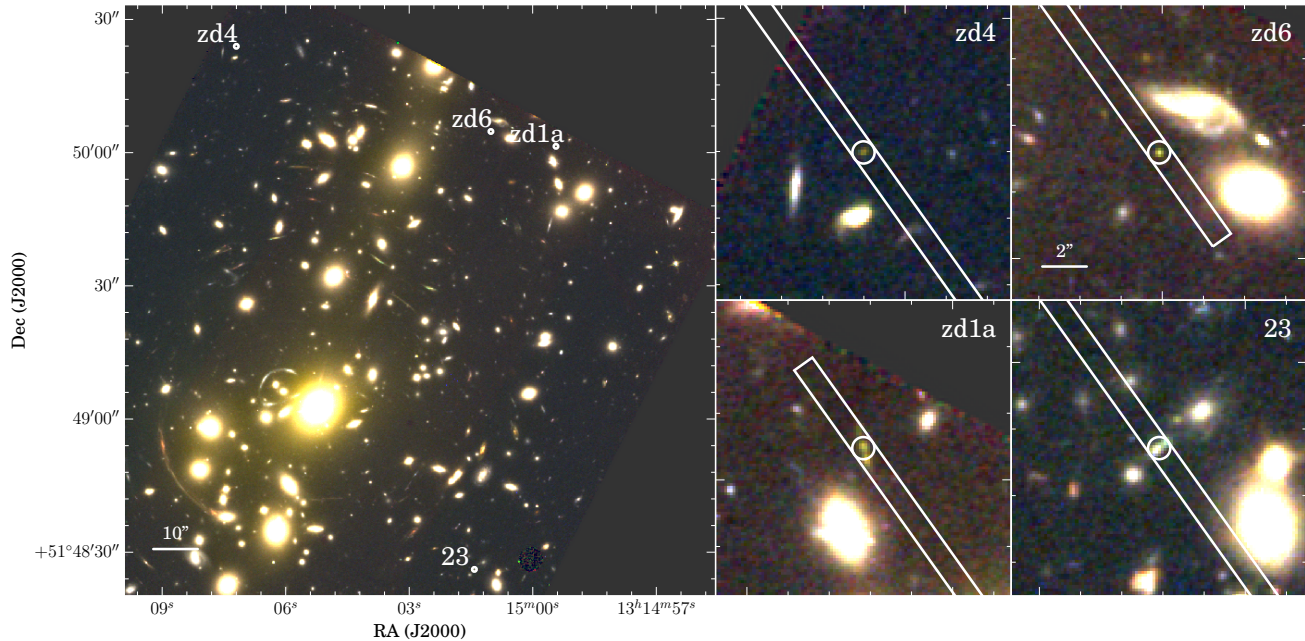


Figure 1. Overview of the Keck/MOSFIRE J-band observations of four gravitationally-lensed galaxies at $5.8 < z < 7.0$ in the field of Abell 1703. Positions of the galaxies are overlaid on the HST color image (z_{850} , J_{125} , H_{160} -bands) of the cluster. The right panel shows a zoomed in view. Information on the galaxies and MOSFIRE spectra is presented in §3.

3 RESULTS

In the following, we discuss the physical properties of each of the four galaxies that form the basis of this study and report the detections and non-detections arising from the MOSFIRE spectra.

3.1 A1703-zd6

A1703-zd6 is a bright ($H=25.9$) z -band dropout first identified in Bradley et al. (2012). A spectroscopic redshift ($z = 7.045$) was achieved via detection of $\text{Ly}\alpha$ at 9780 \AA (Schenker et al. 2012). The absolute UV magnitude is found to be $M_{\text{UV}} = -19.3$ after correcting for the source magnification ($\mu = 5.2$).

The MOSFIRE J-band spectrum of A1703-zd6 covers 1.1530 to $1.3519 \mu\text{m}$ providing spectral coverage between 1433 \AA and 1680 \AA in the rest-frame, enabling constraints on the strength of [NIV], CIV, He II, and OIII]. The $\text{Ly}\alpha$ redshift (Schenker et al. 2012) allows us to predict the window over which these lines will be located. In doing so, we must account for the velocity offset between $\text{Ly}\alpha$ and the other FUV lines. We expect the [NIV], [CIII], and OIII] doublets to trace the systemic redshift (Vanzella et al. 2010; Stark et al. 2014a) and $\text{Ly}\alpha$ to be redshifted between 0 and 450 km s^{-1} with respect to the systemic redshift. The CIV λ 1549 doublet is a resonant line and may also appear redshifted with respect to the other FUV metal lines.

The CIV doublet is easily resolved by MOSFIRE at $z \simeq 7$. If CIV traces gas at the same redshift as $\text{Ly}\alpha$ ($z = 7.045 \pm 0.003$), we would expect CIV λ 1548 to be located between 1.2450 and $1.2460 \mu\text{m}$ and CIV λ 1550 between 1.2471 and $1.2481 \mu\text{m}$. As can be seen in the 2D spectrum shown in Figure 2, CIV λ 1548 is confidently detected in the window defined by $\text{Ly}\alpha$ at $1.2458 \mu\text{m}$. CIV λ 1550 is also likely detected at $1.2474 \mu\text{m}$. A skyline redward of the line makes determination of the exact centroid difficult. The CIV λ 1548 line flux is $4.1 \pm 0.8 \times 10^{-18} \text{ erg cm}^{-2} \text{ s}^{-1}$. Determi-

nation of the CIV λ 1550 flux is more difficult because of the neighbouring sky line. We measure a line flux of $3.8 \pm 0.8 \times 10^{-18} \text{ erg cm}^{-2} \text{ s}^{-1}$ blueward of the skyline. Taking into account the seeing and the fraction of the galaxy covered by the MOSFIRE slit, we estimate that an aperture correction of $1.2\times$ must be applied to the line flux for accurate equivalent width measurements. Applying this correction, we derive rest-frame equivalent widths of $19.9 \pm 4.2 \text{ \AA}$ and $18.1 \pm 4.3 \text{ \AA}$ for the CIV λ 1548 and CIV λ 1550 components, respectively. The observed spectral FWHM of CIV λ 1548 (5.2 \AA) is identical to the FWHM of nearby sky lines indicating that the line is narrow and unresolved with a velocity FWHM of $\lesssim 125 \text{ km s}^{-1}$.

To predict the wavelengths of the OIII] λ 1660,1666 doublet, we consider $\text{Ly}\alpha$ velocity offsets ($\Delta v_{\text{Ly}\alpha}$) between 0 and 450 km s^{-1} , consistent with observations of $z \simeq 2$ galaxies (Tapken et al. 2007; Steidel et al. 2010). Under these assumptions, the OIII] λ 1660 line will lie between $1.3341 \mu\text{m}$ ($\Delta v_{\text{Ly}\alpha} = 450 \text{ km s}^{-1}$) and $1.3361 \mu\text{m}$ ($\Delta v_{\text{Ly}\alpha} = 0 \text{ km s}^{-1}$). An emission feature is visible in this spectral window at $1.3358 \mu\text{m}$ (Figure 2). We tentatively identify this line as OIII] λ 1660. After accounting for the aperture correction, the measured line flux ($1.8 \pm 0.7 \times 10^{-18} \text{ erg cm}^{-2} \text{ s}^{-1}$) implies a rest-frame equivalent width of $9.8 \pm 3.9 \text{ \AA}$.

Since CIV and $\text{Ly}\alpha$ are both resonant transitions, OIII] λ 1660 provides the only constraint on the systemic redshift. From the peak flux of emission feature, we estimate a redshift of $z_{\text{sys}} = 7.0433$. The $\text{Ly}\alpha$ velocity offset that would be implied by this tentative detection, $\Delta v_{\text{Ly}\alpha} = 60 \text{ km s}^{-1}$, suggests $\text{Ly}\alpha$ is emerging close to systemic redshift. A more robust detection is required to verify the $\text{Ly}\alpha$ velocity offset. But we note that this measurement would be consistent with both $\text{Ly}\alpha$ emitting galaxies at $z \simeq 2$ (Tapken et al. 2007; McLinden et al. 2011; Hashimoto et al. 2013). Such small velocity offsets appear to be more common at higher redshifts

Line	λ_{rest} (Å)	λ_{obs} (Å)	Line Flux (10^{-18} erg cm $^{-2}$ s $^{-1}$)	W_0 (Å)
Ly α [†]	1215.67	9780	28.4 ± 5.3	65 ± 12
NIV]	1483.3	...	<3.6	<15.7
...	1486.5	...	<4.3	<19.0
CIV	1548.19	12457.9	4.1 ± 0.8	19.9 ± 4.2
...	1550.77	12473.5	3.8 ± 0.8	18.1 ± 4.3
He II	1640.52	...	<2.1	<11.4
OIII]	1660.81	13358.3	1.8 ± 0.7	9.8 ± 3.9
...	1666.15

Table 2. Emission line properties of the $z_{Ly\alpha} = 7.045$ galaxy A1703-zd6 (Bradley et al. 2011). An aperture correction of $1.20\times$ must be applied to the emission line fluxes if computing line luminosities. The † next to Ly α notes that this flux measurement is from Schenker et al. (2012). The OIII] λ 1666 emission line is obscured by a skyline. The equivalent widths include the aperture correction and are quoted in the rest-frame. The limits are 2σ .

(Schenker et al. 2013a; Stark et al. 2014a), consistent with the rising fraction of Ly α emitting galaxies with redshift over $3 < z < 6$ (Stark et al. 2011). As discussed in Choudhury et al. (2014), existence of small Ly α velocity offsets at $z \gtrsim 6$ reduces the IGM neutral hydrogen fraction required to explain the rapid attenuation of Ly α over $6 < z < 7$.

At $z = 7.0433$, the OIII] λ 1666 is located on top of a strong skyline at $1.340\mu\text{m}$ (Figure 2) and is not detected in the MOSFIRE spectrum. We also do not detect He II λ 1640 or NIV] λ 1483,1487. Flux and equivalent width limits (2σ) are provided in Table 2. Non-detection of He II and NIV] is consistent with the emission line spectra of $z \simeq 1.5 - 3$ metal poor dwarf galaxies (Christensen et al. 2012; Stark et al. 2014b). In these systems, the FUV metal lines (CIV, CIII], OIII]) are typically much stronger than He II and NIV]. The 2σ upper limit on the He II to Ly α flux ratio (<0.07) is nevertheless consistent with the spectrum of BX 418 ($f_{HeII}/f_{Ly\alpha} = 0.03$), a metal poor $z = 2.3$ galaxy discussed in detail in Erb et al. (2010). A deeper J-band spectrum of A1703-zd6 would be required to determine if He II is present at a similar flux as BX 418.

3.2 A1703-zd1a

A1703-zd1a is a very bright ($H=23.9$) z -band dropout. After correcting for its lensing magnification ($\mu = 9.0 \pm 4.5$; Bradley et al. 2011), the absolute magnitude ($M_{UV} = -20.6$) of A1703-zd1a is found to be identical to L_{UV}^* at $z \simeq 6.8$ (Bouwens et al. 2014b). The UV slope ($\beta = -1.4$; Smit et al. 2014) is redder than average for L_{UV}^* z -drops (Bouwens et al. 2014a). Measurement of the Spitzer/IRAC [3.6]-[4.5] color reveals a strong flux excess in [3.6], suggestive of strong [OIII]+H β line contamination (Smit et al. 2014). This likely places the galaxy in the redshift range $z = 6.6 - 6.9$ where [OIII]+H β is in [3.6] and H α is between the [3.6] and [4.5] filters. In this redshift range, the MOSFIRE J-band spectrum is sensitive to emission from CIV, He II, and OIII]. Since both components of CIV and OIII] are resolved, there are up to five emission lines which could be visible in the spectrum.

Examination of the MOSFIRE spectrum reveals no features as strong as the CIV λ 1548 line in A1703-zd6. In regions between sky lines, the 5σ upper limit to the line flux is 3.0×10^{-18} erg cm $^{-2}$ s $^{-1}$. Given the seeing, slit width, and source size, we estimate an aperture correction of $1.27\times$ is required for comparison of line fluxes to the total continuum flux densities. Applying this correction factor to the line flux limit, we derive a 5σ rest-frame

equivalent width limit of 2.3 \AA , considerably lower than that seen in the spectrum of A1703-zd6. The spectrum is sensitive to CIV over $6.4 < z < 7.7$, covering the entire redshift range suggested by the photometric redshift.

3.3 A1703-zd4

A1703-zd4 is another bright ($H_{160}=25.4$) z -band dropout galaxy identified in Bradley et al. (2012). The broadband SED is best fit by a redshift of $z = 8.4$ with acceptable solutions ranging between $z = 7.0$ and $z = 9.3$ (Bradley et al. 2012). After taking into account the source magnification ($\mu = 3.1$), the absolute magnitude of A1703-zd4 is $M_{UV} = -20.6$ at its best fit photometric redshift. The J-band MOSFIRE spectrum is sensitive to Ly α over the redshift range $8.5 < z < 10.1$ and CIV over $6.4 < z < 7.7$.

We have visually examined the spectrum for potential emission features. While several low S/N features are present, no definitive redshift identification is possible with the current spectrum. Conservatively assuming a line width of 10 \AA (twice the value of the CIV λ 1548 line in A1703-zd6) and $1''$ aperture along the slit, we find that typical 5σ line flux limits are 2.6×10^{-18} erg cm $^{-2}$ s $^{-1}$ in between OH sky lines. Taking into account the seeing, slit width, and galaxy size, we compute an aperture correction of $1.21\times$. Applying this correction to the line flux limit and using the J $_{125}$ -band magnitude from Bradley et al. (2012) as the continuum flux density at 1.15 - $1.35\mu\text{m}$, we derive a rest-frame equivalent width limit of $\simeq 6 \text{ \AA}$ for regions between OH lines. With the resolution provided by MOSFIRE, the incidence of OH lines is minimized, but nonetheless roughly 40% of the J-band spectral window is still impacted by sky lines so it is of course possible that an emission line from A1703-zd4 is obscured by a bright skyline.

Additional spectroscopy will help clarify the redshift of A1703-zd4, as the current J-band exposure only samples a portion of the photometric redshift distribution function. A Y-band spectrum would extend the Ly α coverage down to the redshift range $7.0 < z < 8.2$, while an H-band spectrum of A1703-zd4 would extend the redshift range over which FUV metal lines are detectable.

3.4 A1703-23

A1703-23 was identified as a bright ($H=23.75$) i -band dropout and spectroscopically-confirmed in Richard et al. (2009). Ly α was detected in an optical spectrum at 8300.5 \AA implying a redshift of $z = 5.828$, consistent with expectations from the SED. Richard et al. (2009) measure a Ly α flux of 2.5×10^{-17} erg cm $^{-2}$ s $^{-1}$. After correcting for the magnification factor estimated by Richard et al. (2009), $\mu = 3$, the UV absolute magnitude of A1703-23 is found to be $M_{UV} = -21.7$, corresponding to a 1.6 - $2.0L_{UV}^*$ galaxy at $z \simeq 5.9$ (Bouwens et al. 2014b). Similar to A1703-zd1a, the UV spectral slope of A1703-23 ($\beta = -1.5$) is redder than typical i -band dropouts. Since the continuum is not detected in the optical spectrum, we estimate the Ly α equivalent width from the broadband flux measurements. We use the UV spectral slope to convert the J-band flux to a continuum flux at the wavelength of Ly α . Following this procedure, we estimate a rest-frame equivalent width of $W_{Ly\alpha}=10.3 \text{ \AA}$ for A1703-23.

Using the Ly α spectroscopic redshift, we predict the observed wavelengths over which the CIII] doublet will be located. Studies at lower redshift demonstrate that CIII] tends to trace the systemic redshift (Stark et al. 2014b). Allowing for the characteristic Ly α velocity offset of 0 to 450 km s^{-1} with respect to

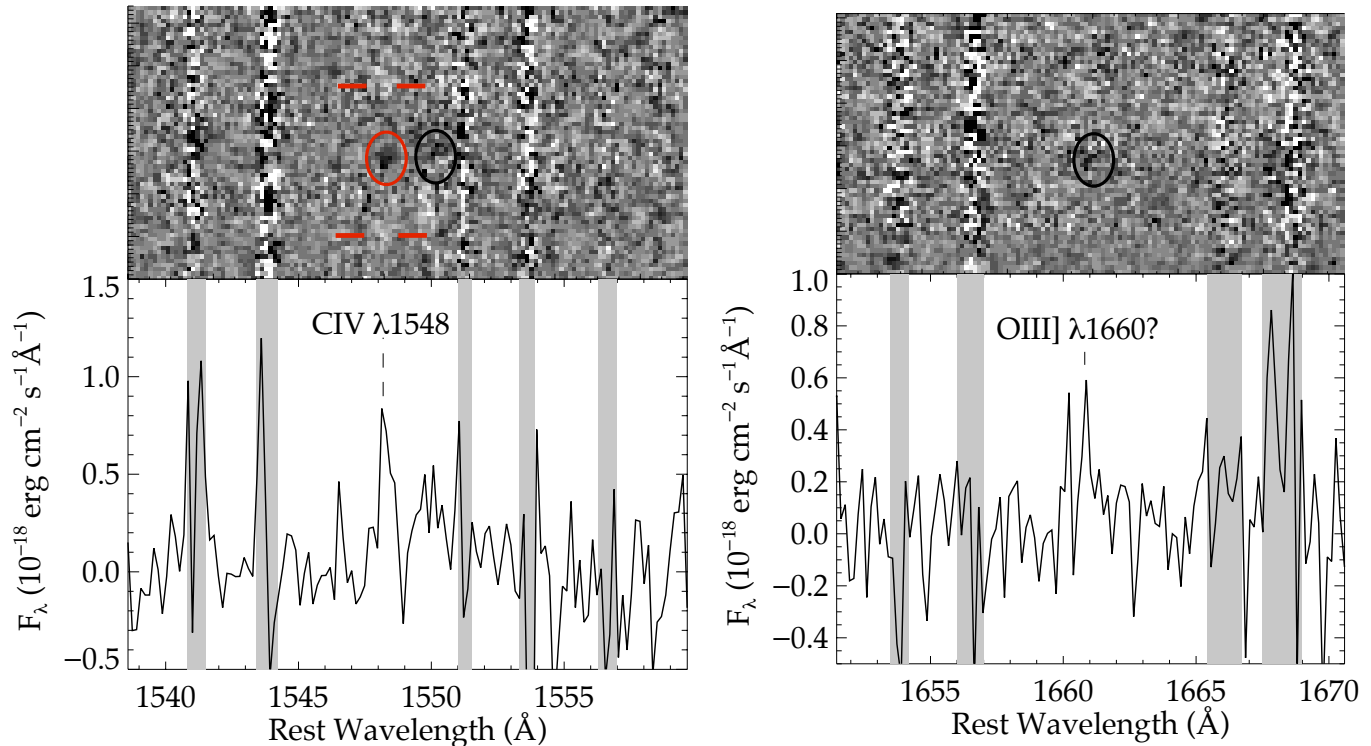


Figure 2. Keck/MOSFIRE J-band spectrum of the gravitationally-lensed $z_{\text{Ly}\alpha} = 7.045$ galaxy A1703-zd6. The spectroscopic redshift was known prior to MOSFIRE observations from Ly α emission (Schenker et al. 2012). Top panels show the two-dimensional (unsmoothed) spectra with black showing positive emission. The red oval identifies the emission feature at the rest-frame wavelength expected for CIV λ 1548. The characteristic negative emission from the dither pattern is demarcated by red horizontal lines. Black ovals highlight the expected location of CIV λ 1550 (left panel) and OIII] λ 1660 (right panel). The one-dimensional extracted spectra are shown below. Vertical grey swaths indicate regions of elevated noise from OH sky lines.

the systemic redshift, we predict that [CIII] λ 1907 will lie between 1.2999 and 1.3019 μm and CIII] λ 1909 will be located between 1.3013 and 1.3033 μm . The flux ratio of [CIII] λ 1907 and CIII] λ 1909 is set by the electron density in the gas traced by doubly-ionized carbon. In high redshift galaxies, observations indicate [CIII] λ 1907/CIII] λ 1909 flux ratios in the range 1.2-1.6 (Hainline et al. 2009; James et al. 2014).

As can be seen in the the 2D spectrum (Figure 3), no strong emission lines are detected. The region over which [CIII] λ 1907 is expected is almost entirely devoid of OH sky lines. If we conservatively assume a FWHM of 10 \AA (roughly $2\times$ as large as the unresolved CIV line in A1703-zd6), we find that the 5σ limit on the [CIII] λ 1907 line flux would be 2.5×10^{-18} $\text{erg cm}^{-2} \text{s}^{-1}$. Roughly 70% of the CIII] λ 1909 spectral window is clean with a 5σ flux limit of 5.6×10^{-18} $\text{erg cm}^{-2} \text{s}^{-1}$. The CIII] λ 1909 flux limit is slightly larger because the adopted 10 \AA line width overlaps with the OH line. Applying an aperture correction of $1.66\times$ (calculated from the seeing, slit width, and source size), we derive 5σ rest-frame equivalent width limits of 1.9 \AA for [CIII] λ 1907 and 4.3 \AA for CIII] λ 1909. Detection of both components of the doublet would require a total equivalent width in excess of 6.2 \AA .

The non-detection of CIII] in A1703-23 is consistent with the physical picture presented in Stark et al. (2014b). At intermediate redshifts, the CIII] equivalent width is found to increase with the Ly α equivalent width. For galaxies with Ly α equivalent widths similar to the moderate value observed in A1703-23, CIII] equivalent widths are seen to be in the range $W_{\text{CIII]}} \simeq 2\text{-}4$ \AA (Shapley

et al. 2003; Stark et al. 2014b), below the equivalent width limit provided by the MOSFIRE spectrum. However recent studies have demonstrated that some galaxies at $z \simeq 6\text{--}7$ have UV metal lines that are stronger than found in the intermediate redshift samples. The non-detection of CIII] in A1703-23 suggests that not all $z \gtrsim 6$ galaxies have such extreme rest-UV spectra.

4 A HARD IONIZING SPECTRUM AT $Z = 7$

Here we use photoionization models to characterize the shape of the ionizing spectrum required to produce the observed spectral properties of A1703-zd6. We explore galaxy models with stellar input spectra in §4.1 and AGN models in §4.2.

4.1 Stellar models

We fit the observed CIV λ 1548 emission equivalent width (the component of the doublet that is most robustly detected) and broadband F125W and F160W fluxes of the galaxy using an approach similar to that adopted in Stark et al. (2014b). This is based on a combination of the latest version of the Bruzual & Charlot (2003) stellar population synthesis model with the standard photoionization code CLOUDY (Ferland et al. 2013) to describe the emission from stars and the interstellar gas (Gutkin et al., in preparation, who follow the prescription of Charlot & Longhetti 2001).

We adopt the same parameterization of interstellar gas and

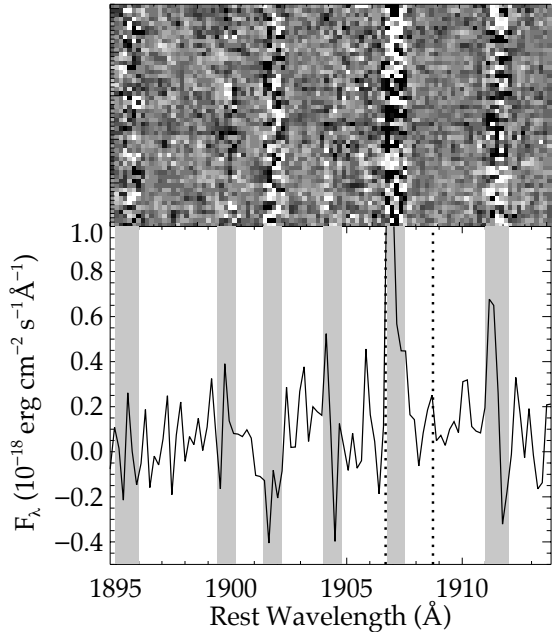


Figure 3. Non-detection of [CIII]λ1907, CIII]λ1909 doublet in a Keck/MOSFIRE J-band spectrum of the spectroscopically-confirmed $z = 5.828$ galaxy A1703-23 (see §3.4 for details). Top panel shows the two-dimensional (unsmoothed) spectra with black corresponding to positive emission. The one-dimensional extracted spectra is shown below. Vertical grey swaths indicate regions of elevated noise from OH sky lines, and vertical dotted lines show expected location of CIII] doublet at the redshift of Ly α .

dust as in Stark et al. (2014a), to whom we refer for detail. In brief, the main adjustable parameters of the photoionized gas are the interstellar metallicity, Z , the typical ionization parameter of a newly ionized HII region, U (which characterizes the ratio of ionizing-photon to gas densities at the edge of the Strömgren sphere), and the dust-to-metal (mass) ratio, ξ_d (which characterizes the depletion of metals on to dust grains). We consider here models with hydrogen densities ranging between 100 and 1000 cm^{-3} and C/O (and N/O) abundance ratios ranging from 1.0 to 0.1 times the standard values in nearby galaxies [$(\text{C}/\text{O})_{\odot} \approx 0.44$ and $(\text{N}/\text{O})_{\odot} \approx 0.07$]. We also include attenuation of line and continuum photons by dust in the neutral ISM, using the 2-component model of Charlot & Fall (2000), as implemented by da Cunha et al. (2008, their equations 1–4). This is parameterized in terms of the total V -band attenuation optical depth of the dust, $\hat{\tau}_V$, and the fraction μ of this arising from dust in the diffuse ISM rather than in giant molecular clouds. Accounting for these two dust components is important to describe the different attenuation of emission-line and stellar continuum photons. We use a comprehensive model grid similar to that adopted by Stark et al. (2015)

As in Stark et al. (2014a), we consider models with 2-component star formation histories: a ‘starburst’ component (represented here by a 3 Myr-old stellar population with constant SFR) and an ‘old’ component (represented by a stellar population with constant or exponentially declining SFR with age between 10 Myr and the age of the Universe at the galaxy redshift, i.e. 0.75 Gyr). We adopt a standard Chabrier (2003) initial mass function and the same stellar metallicity for both components, which also coincides with the current interstellar metallicity of the galaxy.

A1703-zd6	
$\log U$	$-1.35^{+0.24}_{-0.40}$
$12 + \log (\text{O}/\text{H})$	$7.05^{+0.31}_{-0.25}$
$\log(\xi_{\text{ion}}/\text{Hz erg}^{-1})$	$25.68^{+0.27}_{-0.19}$
$W(\text{Ly}\alpha)$	$2.06^{+0.33}_{-0.24}$
$\log(\text{NV } 1240/\text{CIV } 1548)$	$-2.43^{+0.42}_{-0.42}$
$\log(\text{HeII } 1640/\text{CIV } 1548)$	$-1.59^{+0.22}_{-0.20}$
$\log(\text{MgII } 2798/\text{CIV } 1548)$	$-1.95^{+0.42}_{-0.47}$

Table 3. A1703-zd6 photoionization modelling results. The input spectra to the photoionization code are from the latest version of the Bruzual & Charlot (2003) stellar population synthesis models. We fit the CIVλ1548 equivalent width and J_{125} and H_{160} broadband flux densities.

To interpret the combined stellar and nebular emission from the galaxy, we use the same Bayesian approach as in Stark et al. (2015; see also equation 2.10 of Pacifici et al. 2012) and a grid of models covering wide ranges in the above parameters. In practice, we find that the requirement to reproduce the strong CIV1548 emission equivalent width implies that the best-fit models are entirely dominated by the young stellar component (for reference, the best-fit model equivalent width for this line is 19.9 Å). Such models also provide excellent fits to the observed F125W and F160W fluxes (with a dust attenuation optical depth consistent with zero). Also, since nebular emission is constrained only by the equivalent width of a single component of the CIV doublet in our analysis, the resulting constraints on the gas density and C/O ratio are extremely weak.

The models demonstrate that the CIV emission line strength of A1703-zd6 can be reproduced by stellar input spectra. The range of acceptable model parameters is shown in Table 3. Models that fit the observed spectral properties have a large ionization parameter ($\log U = -1.35$) and very low metallicity ($12 + \log \text{O}/\text{H} = 7.05$). The production rate of hydrogen ionizing photons per observed (i.e. attenuated) 1500 Å luminosity is very large ($\log(\xi_{\text{ion}}/\text{erg}^{-1}\text{Hz})=25.68$) in models that reproduce the data. We note that we do not attenuate the ionizing photon output in our calculation of ξ_{ion} , as our primary goal is to be able to predict how many hydrogen ionizing photons were produced based on the observed 1500 Å luminosity.

The ionizing spectrum of the best-fitting stellar model (Figure 4) reveals a significant flux of energetic radiation at 40-50 eV capable of producing nebular CIV emission. The flux density drops off significantly above ~ 54 eV, resulting in much weaker emission from He II and NV. Stellar models predict NVλ1240 and He IIλ1640 fluxes that are 30-250× weaker than the CIVλ1548 line strength (Table 3). These lines are unlikely to be detected if the CIV emission is powered by a stellar population.

4.2 AGN models

We also explore a comparison of A1703-zd6 to AGN photoionization models. We use the models of Feltre et al. 2015 in prep., which represent the narrow line emission region (NLR) of the AGN and have been realized with the photoionization code CLOUDY (latest version C13.03, last described in Ferland et al. 2013). The solar abundance and dust depletion values are the same as those used in the models for star-forming galaxies used in §4.1 and developed by Gutkin et al. 2015, in prep. The input parameters for the AGN NLR models are taken to be the interstellar metallicity, Z , in the range between 0.0001 and 0.05, the dust-to-metal(mass) ratio, $\xi_d = 0.1, 0.3$

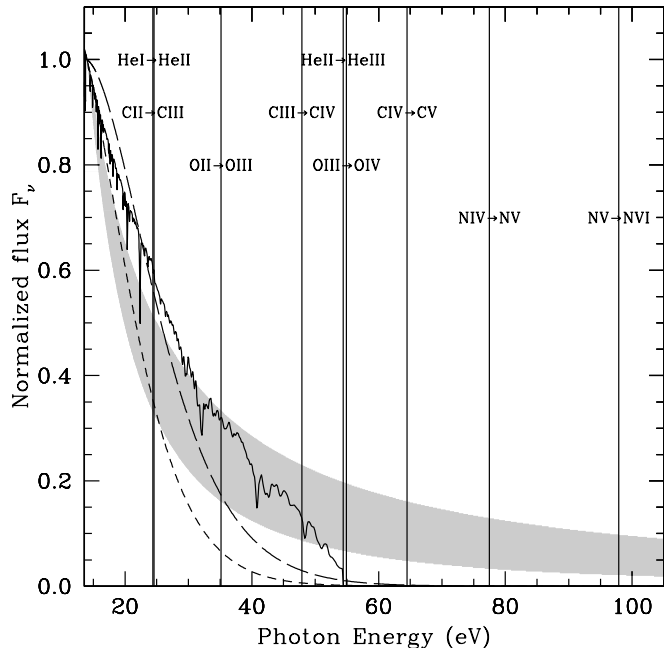


Figure 4. Ionizing spectra from different sources, plotted together with the ionizing potentials of different ions (vertical lines). The solid spectral energy distribution corresponds to the best-fit galaxy model reported in Section §4, while the shaded area shows the range in ionizing spectra produced by $F_\nu \propto \nu^\alpha$ AGN models with spectral indices between $\alpha = -1.2$ (upper ridge) and -2.0 (lower ridge). For comparison to the radiation field in typical galaxies at $z \simeq 2$ (Steidel et al. 2014), we also display blackbody spectra with temperatures of 45,000 (short dashed) and 55,000 K (long dashed), respectively. All spectra are normalized to unity at 13.6 eV.

and 0.5, the hydrogen density, $n_{\text{H}} = 10^2, 10^3$ and 10^4 cm^{-3} , and the ionization parameter, U , in the range $\log U = -5$ to -1 . The AGN is characterised by a power law $F_\nu \propto \nu^\alpha$, with spectral indices $\alpha = -1, 2, -1.4, -1.7$ and -2.0 in the wavelength range between 0.001 and $0.25 \mu\text{m}$. For completeness, we include the effects of attenuation using the prescription of Calzetti et al. (2000).

In contrast to the stellar model fits (§4.1), we do not include the constraints from the line equivalent widths and broadband photometry because of the arbitrary scaling of the AGN and host galaxy luminosities that would be required to model the underlying continuum. The AGN fit is instead focused on the two most robustly constrained flux ratios, namely $\text{OIII}\lambda 1660/\text{CIV}\lambda 1548$ and $\text{HeII}\lambda 1640/\text{CIV}\lambda 1548$. Given the tentative nature of the $\text{OIII}\lambda 1660$ detection, we adopt a 5σ upper limit ($<3.5 \times 10^{-18} \text{ erg cm}^{-2} \text{ s}^{-1}$) to the line flux. We note that this limit is consistent with the observed faint flux level of the possible emission feature ($1.8 \times 10^{-18} \text{ erg cm}^{-2} \text{ s}^{-1}$). The measurement of $\text{CIV}\lambda 1548$ and upper limits on $\text{OIII}\lambda 1660$ and $\text{HeII}\lambda 1640$ thus translate into upper limits for the emission line ratios $\text{OIII}\lambda 1660/\text{CIV}\lambda 1548$ and $\text{HeII}/\text{CIV}\lambda 1548$ used in the fit.

The fitting procedure demonstrates that the existing observational constraints are also marginally consistent with photoionization by an AGN. The two flux ratio limits favour best-fit AGN models corresponding to metallicity and hydrogen density of $Z=0.001$ and 10^2 cm^{-3} , respectively. The ionizing spectra of acceptable AGN models is shown in Figure 4. The AGN power law spectrum has considerably greater flux than the galaxy models at energies in excess of 50 eV. As a result, AGN models predict stronger He

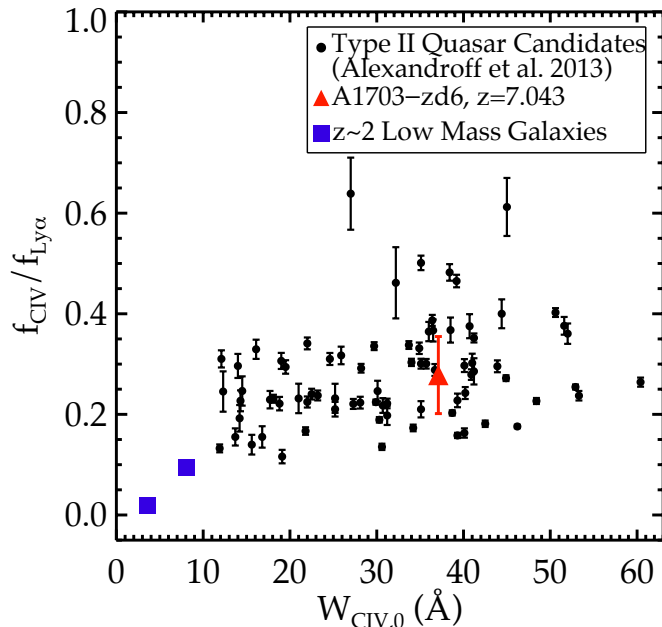


Figure 5. Comparison of the CIV/Ly α flux ratio in A1703-zd6 with type II quasar candidates at $2 < z < 4.3$ and low mass metal poor galaxies at $z \simeq 2$. The quasar candidates were reported in Alexandroff et al. (2013) and the low mass $z \simeq 2$ galaxies are CIV emitters from Stark et al. (2014b). The CIV emitting strength of A1703-zd6 is comparable to that seen in AGN spectra and is more extreme than in powerful line emitting galaxies at lower redshift.

$\text{II}\lambda 1640$ than the galaxy models discussed in §4.2, with a flux that is 40% that of the measured $\text{CIV}\lambda 1548$ flux. Current limits suggest the He II flux is less than 50% that of $\text{CIV}\lambda 1548$ at 2σ . Deeper J-band observations may thus be able to detect He II if A1703-zd6 is powered by an AGN.

5 DISCUSSION

5.1 Comparison to UV Radiation Field at Lower Redshifts

Nebular CIV emission is seldom detected in $z \simeq 2 - 3$ galaxies. Instead the CIV profile shows strong absorption from highly ionized outflowing gas superimposed on a P-Cygni profile from stellar winds (e.g. Shapley et al. 2003). The absence of strong CIV emission in typical galaxies points to a negligible output of photons with energies greater than 47.9 eV, consistent with the radiation field expected from the blackbody models predicted for $z \simeq 2$ galaxies in Steidel et al. (2014). In Figure 4, we overlay the $z \simeq 2$ galaxy ionizing spectrum on the AGN and stellar photoionization models which reproduce the spectral features of A1703-zd6. Both models predict that the $z = 7.045$ galaxy must have a larger output of 20-50 eV radiation than is commonly seen in $z \simeq 2 - 3$ galaxies.

When strong CIV emission is present in lower redshift systems, it is generally thought to reflect AGN activity. At $z \simeq 2 - 3$, AGNs with narrow emission lines (FWHM less than 2000 km s^{-1}) comprise only 1% of UV-selected galaxy samples (Steidel et al. 2002; Hainline et al. 2011). In these systems, the CIV flux is typically 20% that of Ly α , with equivalent widths ranging between 10 and 50 Å (Steidel et al. 2002; Hainline et al. 2011; Alexandroff et al. 2013), comparable to what is observed in A1703-zd6 (Figure

5). Nebular He II is often seen in UV-selected narrow-lined AGNs, but the equivalent width is only 5-10 Å (Hainline et al. 2011), also consistent with the non-detection of He II in A1703-zd6. While the line properties of A1703-zd6 and UV-selected AGNs appear similar, the continuum shapes are very different. Hainline et al. (2011) demonstrated that at lower redshift, the UV continuum power-law slope of the UV-selected AGNs ($\beta = -0.3$) tends to be much redder than non-AGNs ($\beta = -1.5$). In contrast, A1703-zd6 has a very blue ($\beta = -2.4$) continuum slope (Bradley et al. 2012; Schenker et al. 2012), similar to the parent population of galaxies at $z \simeq 7$ (e.g., Bouwens et al. 2014a).

Among star forming galaxies with low stellar masses (10^6 - $10^9 M_{\odot}$), nebular CIV emission is more common (Christensen et al. 2012; Stark et al. 2014b). These systems tend to have blue colours, large specific star formation rates, and prominent Ly α emission lines. The strong CIV emission is thought to reflect an intense radiation field from massive stars following a recent upturn in star formation (Stark et al. 2014b). Given the similarly low masses, blue colours, and large specific star formation rates of reionization-era galaxies, it is possible that nebular CIV emission might be more common in $z > 6$ galaxies. Yet as is evident in Figure 5, the CIV equivalent widths and CIV/Ly α flux ratios of A1703-zd6 are 5-10 \times larger than the low mass samples at lower redshift. We note that the reduced CIV/Ly α flux ratio of A1703-zd6 with respect to $z \simeq 2$ systems could be in part due to suppression of Ly α emission by the IGM or optically thick absorbers. But given the very large rest-frame Ly α equivalent width of this system (65 Å, Schenker et al. 2012), IGM attenuation is not likely to be the primary factor responsible for the nearly order of magnitude offset in the CIV/Ly α ratio compared to the lower redshift systems.

There does not appear to be a completely analogous population to A1703-zd6 at lower redshift. Deeper spectroscopic constraints on other ultraviolet spectral features (NV, He II, CIII]) will help characterize the powering mechanism. Another crucial step will be determining whether systems like A1703-zd6 are common at $z \simeq 7$. The only other galaxy in our sample with a redshift which places CIV in the spectral window we targeted is A1703-zd1a (§3.2). The non-detection of CIV in this system suggests that the line is not strong in all $z \simeq 7$ galaxies. But presence of nebular CIV emission in one of two galaxies we observed represents a significant departure from the 1% detection rate at lower redshift. If the galaxies in our sample are typical of the UV-selected population at $z \simeq 7$, it would suggest a very different UV radiation field is present in many early star forming systems, potentially altering our current picture of the contribution of galaxies to reionization (e.g., Robertson et al. 2015, Bouwens et al. 2015). If the duty cycle associated with the intense radiation field is large (such that A1703-zd6 is not a bursty outlier), then it would be possible to achieve reionization by $z \simeq 6$ while adopting a lower ionizing photon escape fraction (f_{esc}) or a brighter absolute magnitude limit when integrating the UV luminosity function.

5.2 Nature of $z > 7$ Ly α emitters

Currently all $z > 7$ UV metal line detections come from galaxies with previously known Ly α detections. This largely reflects our selection criteria, as we have primarily focused our follow-up on known Ly α emitters. The spectroscopic redshifts provided by Ly α are very useful, allowing us to ensure that UV metal lines are located at wavelengths which are unobscured by the atmosphere. But given the unusually strong CIV emission, we must consider

whether our pre-selection of Ly α emitters might have biased us toward locating galaxies with extreme radiation fields.

While Ly α emission is very common among $z \simeq 6$ galaxies (Stark et al. 2011), it is exceedingly rare at $z \simeq 7$ (e.g., Treu et al. 2013; Schenker et al. 2014; Tilvi et al. 2014). The weak Ly α emission is thought to reflect an increase in the IGM neutral hydrogen fraction over $6 < z < 8$ (Mesinger et al. 2015; Choudhury et al. 2014), as would be expected if reionization is incomplete at $z \simeq 7-8$ (e.g. Robertson et al. 2013, 2015). Recent work suggests that an increased incidence of optically thick absorbers may also contribute to the attenuation of Ly α (Bolton & Haehnelt 2013), although the importance of such systems remains unclear (Mesinger et al. 2015). Based on this overall picture, galaxies with Ly α detections at $z > 7$, such as A1703-zd6, will be those that are situated in regions of the IGM which have already been ionized.

It is conceivable that the only $z > 7$ galaxies that can be seen in Ly α are those with extreme radiation fields capable of ionizing hydrogen in the IGM and in optically thick absorbers. In this case, the presence of high ionization features like CIV in A1703-zd6 would be a direct consequence of the pre-selection by Ly α . Given the rarity of Ly α emitters at $z > 7$, the hard ionizing spectrum shown in Figure 4 would thus be limited to a small percentage of the early galaxy population. Additional constraints on the strength of high ionization lines in $z > 7$ Ly α emitters will be needed to determine whether the presence of Ly α is indeed linked to the intensity of the radiation field. Likewise, determination of the typical ionizing spectrum will require sampling galaxies with a diverse range of properties, including those without Ly α emission.

5.3 Implications for early galaxy spectroscopy

Recent studies have proposed that the [CIII] λ 1907, CIII] λ 1909 doublet provides a feasible route toward spectroscopic confirmation of reionization-era galaxies in which Ly α is strongly attenuated by the partially neutral IGM (Erb et al. 2010; Stark et al. 2014b). The line may provide a valuable spectroscopic probe of the most distant galaxies that the James Webb Space Telescope (JWST) will find, as the strong rest-optical lines shift out of the spectral window of NIRSPEC at $z \simeq 11$. For future ground-based optical/infrared telescopes, CIII]) may be brightest spectral lines in reionization-era systems. But because of atmospheric absorption in the near-infrared, ground-based facilities will not be able to detect CIII]) emission throughout substantial redshift intervals in the reionization era. The low atmospheric transmission between the J and H-band and H and K_s-band causes CIII]) to be attenuated in galaxies at $5.8 \lesssim z \lesssim 6.9$ and $8.3 \lesssim z \lesssim 10$, respectively (Figure 6).

The presence of CIV and tentative identification of OIII]) in A1703-zd6 suggests that a variety of FUV lines may be present in deep near-infrared spectra of a subset of bright $z > 6$ galaxies. While it is possible that A1703-zd6 may have atypically strong CIV emission (see §5.2), both CIV and OIII]) emission are commonly detected in the spectra of intermediate redshift metal poor galaxies (Erb et al. 2010; Christensen et al. 2012; Stark et al. 2014b). Importantly, both lines are detectable at redshifts where CIII]) is unobservable. CIV can be seen in galaxies over $6.6 < z < 7.4$ (J-band), and $8.7 < z < 10.5$ (H-band), while OIII]) can be identified in galaxies at $6.0 < z < 6.8$ and $8.0 < z < 9.7$ (Figure 6).

The redshift-dependent visibility of the FUV metal lines shown in Figure 6 has implications for the optimal strategy of spectroscopically following up early star forming systems. Of particular interest is the population of extreme [OIII]) $+$ H β emitting galaxies identified via blue [3.6]-[4.5] colours (Smit et al. 2014, 2015)

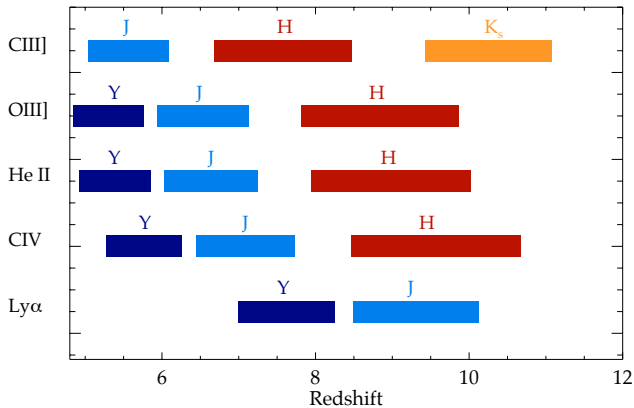


Figure 6. Visibility of FUV lines in $z > 5$ galaxies using ground-based spectrographs. Solid bands give redshift window over which emission lines are detectable in Y, J, H, and K_s -band filters using MOSFIRE on Keck. Atmospheric absorption in the near-infrared limits the redshift range over which any individual spectral feature can be detected.

and thought to lie in the redshift range $z \simeq 6.6 - 6.9$. Stark et al. (2014b) demonstrate that galaxies with extreme optical line emission tend to have large equivalent width FUV metal lines (see Gutkin et al. 2015, in preparation for more details), making this an attractive class of objects to target with rest-frame FUV spectroscopy. However Figure 6 demonstrates that CIII] is likely to be obscured by the atmosphere over some of this redshift range. For the same reason, attempts to identify CIII] emission in $Ly\alpha$ emitters at $z = 6.6$ will not result in many detections. Follow-up efforts of both populations are more likely to succeed by focusing on CIV, He II, and OIII] in the J-band.

6 SUMMARY

We have presented new measurements of various far-ultraviolet emission lines ($Ly\alpha$, CIV, He II, OIII]) in $z \sim 6 - 8$ galaxy spectra. Using the MOSFIRE spectrograph (McLean et al. 2012) on Keck I, we have obtained J-band spectra of four gravitationally lensed galaxies in the massive cluster field Abell 1703 (Table 1). The galaxies are bright ($H=23.8-25.9$) and span a range of redshifts ($5.8 \lesssim z \lesssim 8.0$), $Ly\alpha$ equivalent widths, UV slopes, and continuum luminosities.

We report a 5.1σ detection of nebular CIV λ 1548 emission in A1703-zd6, a $z = 7.045$ spectroscopically-confirmed galaxy. The observed wavelengths of the UV metal lines are accurately known from the $Ly\alpha$ redshift. The rest-frame CIV equivalent width (38.0 Å) and CIV/ $Ly\alpha$ flux ratio (0.3) we infer for A1703-zd6 are similar to those seen in narrow-lined AGNs at lower redshift. The line is unresolved with a FWHM less than 125 km s^{-1} . The presence of CIV requires a surprisingly large output of very energetic radiation capable of triply ionizing carbon. In §4, we demonstrated that the extreme spectral properties of A1703-zd6 can be powered by an AGN or an intense population of young, very hot, metal poor stars. Photoionization models point to an ionizing spectrum that is very different from that inferred for typical $z \simeq 2$ galaxies.

The data provide constraints on UV metal line emission in two other galaxies. The first of these is A1703-zd1a, a z -band dropout thought to lie at $z \simeq 6.6 - 6.9$ (Smit et al. 2014). In

this redshift range, the MOSFIRE observations probe CIV, He II, and OIII]. No secure emission lines are identified throughout the J-band spectrum. Rest-frame equivalent widths greater than 2.3 Å would have been seen at 5σ if located between OH sky lines. The other system is A1703-23, a spectroscopically confirmed galaxy at $z = 5.828$. We report an upper limit of 1.9 Å on [CIII] λ 1907 and 4.3 Å on [CIII] λ 1909 emission. The lack of detectable CIII] emission is consistent with the relationship between CIII] and $Ly\alpha$ equivalent width presented in Stark et al. (2014b).

At lower redshift, nebular CIV emission is seen in only 1% of UV-selected galaxies (Steidel et al. 2002; Hainline et al. 2011). The presence of strong CIV emission in A1703-zd6, one of the first galaxies we targeted is thus rather surprising. One explanation is that radiation fields are more extreme in $z \simeq 7$ galaxies. This may be expected if reionization-era galaxies are commonly caught following a recent upturn or burst of star formation and would indicate that $z > 7$ systems are more efficient ionizing agents than we previously thought. Alternatively, we consider whether the only systems seen in $Ly\alpha$ at $z > 7$ may be those with extreme radiation fields capable of ionizing hydrogen in optically thick absorbers and the surrounding IGM. In this case, the pre-selection of galaxies by their $Ly\alpha$ emission would result in a very biased sample with extreme spectral features. Further constraints on high ionization emission lines in galaxies with and without $Ly\alpha$ should clarify whether systems like A1703-zd6 are ubiquitous at $z > 7$.

ACKNOWLEDGMENTS

We thank Richard Ellis, Dawn Erb, Martin Haehnelt, Juna Kollmeier, Ian McGreer, and Andrei Mesinger for enlightening conversations. DPS acknowledges support from the National Science Foundation through the grant AST-1410155. JR acknowledges support from the European Research Council (ERC) starting grant CALENDs and the Marie Curie Career Integration Grant 294074. SC, JG and AW acknowledge support from the ERC via an Advanced Grant under grant agreement no. 321323 – NEOGAL. This work was partially supported by a NASA Keck PI Data Award, administered by the NASA Exoplanet Science Institute. Data presented herein were obtained at the W. M. Keck Observatory from telescope time allocated to the National Aeronautics and Space Administration through the agency’s scientific partnership with the California Institute of Technology and the University of California. The Observatory was made possible by the generous financial support of the W. M. Keck Foundation. The authors acknowledge the very significant cultural role that the summit of Mauna Kea has always had within the indigenous Hawaiian community. We are most fortunate to have the opportunity to conduct observations from this mountain.

REFERENCES

- Alexandroff R., Strauss M. A., Greene J. E., Zakamska N. L., Ross N. P., Brandt W. N., Liu G., Smith P. S., Ge J., Hamann F., Myers A. D., Petitjean P., Schneider D. P., Yesuf H., York D. G., 2013, MNRAS, 435, 3306
- Atek H., Richard J., Kneib J.-P., Jauzac M., Schaerer D., Clement B., Limousin M., Jullo E., Natarajan P., Egami E., Ebeling H., 2015, ApJ, 800, 18
- Bayliss M. B., Rigby J. R., Sharon K., Wuyts E., Florian M., Gladsters M. D., Johnson T., Oguri M., 2014, ApJ, 790, 144

- Bolton J. S., Haehnelt M. G., 2013, *MNRAS*, 429, 1695
- Bouwens R. J., Illingworth G. D., Oesch P. A., Labbé I., van Dokkum P. G., Trenti M., Franx M., Smit R., Gonzalez V., Magee D., 2014a, *ApJ*, 793, 115
- Bouwens R. J., Illingworth G. D., Oesch P. A., Trenti M., Labbé I., Bradley L., Carollo M., van Dokkum P. G., Gonzalez V., Holwerda B., Franx M., Spitler L., Smit R., Magee D., 2014b, *ArXiv e-prints*
- Bowler R. A. A., Dunlop J. S., McLure R. J., McCracken H. J., Furusawa H., Taniguchi Y., Fynbo J. P. U., Milvang-Jensen B., Le Fevre O., 2014, *ArXiv e-prints*
- Bradley L. D., Bouwens R. J., Zitrin A., Smit R., Coe D., Ford H. C., Zheng W., Illingworth G. D., Benítez N., Broadhurst T. J., 2012, *ApJ*, 747, 3
- Bradley L. D., Zitrin A., Coe D., Bouwens R., Postman M., Balestra I., Grillo C., Monna A., Rosati P., Seitz S., Host O., Lemze D., Moustakas J., Moustakas L. A., Shu X., Zheng W., Broadhurst T., Carrasco M., Jouvel S., Koekemoer A., Medezinski E., Meneghetti M., Nonino M., Smit R., Umetsu K., Bartelmann M., Benítez N., Donahue M., Ford H., Infante L., Jimenez-Teja Y., Kelson D., Lahav O., Maoz D., Melchior P., Merten J., Molino A., 2014, *ApJ*, 792, 76
- Bruzual G., Charlot S., 2003, *MNRAS*, 344, 1000
- Calzetti D., Armus L., Bohlin R. C., Kinney A. L., Koornneef J., Storchi-Bergmann T., 2000, *ApJ*, 533, 682
- Chabrier G., 2003, *PASP*, 115, 763
- Charlot S., Fall S. M., 2000, *ApJ*, 539, 718
- Charlot S., Longhetti M., 2001, *MNRAS*, 323, 887
- Choudhury T. R., Puchwein E., Haehnelt M. G., Bolton J. S., 2014, *ArXiv e-prints*, arxiv:1412.4790
- Christensen L., Richard J., Hjorth J., Milvang-Jensen B., Laursen P., Limousin M., Dessauges-Zavadsky M., Grillo C., Ebeling H., 2012, *MNRAS*, 427, 1953
- Coe D., Zitrin A., Carrasco M., Shu X., Zheng W., Postman M., Bradley L., Koekemoer A., Bouwens R., Broadhurst T., Monna A., Host O., Moustakas L. A., Ford H., Moustakas J., van der Wel A., Donahue M., Rodney S. A., Benítez N., Jouvel S., Seitz S., Kelson D. D., Rosati P., 2013, *ApJ*, 762, 32
- Curtis-Lake E., McLure R. J., Dunlop J. S., Rogers A. B., Targett T., Dekel A., Ellis R. S., Faber S. M., Ferguson H. C., Grogin N. A., Huang K.-H., Kocevski D. D., Koekemoer A. M., Lai K., Robertson B. E., 2014, Submitted to *MNRAS*, arxiv:1409.1832,
- Curtis-Lake E., McLure R. J., Pearce H. J., Dunlop J. S., Cirasuolo M., Stark D. P., Almaini O., Bradshaw E. J., Chuter R., Foucaud S., Hartley W. G., 2012, *MNRAS*, 422, 1425
- da Cunha E., Charlot S., Elbaz D., 2008, *MNRAS*, 388, 1595
- Duncan K., Conselice C. J., Mortlock A., Hartley W. G., Guo Y., Ferguson H. C., Davé R., Lu Y., Ownsworth J., Ashby M. L. N., Dekel A., Dickinson M., Faber S., Giavalisco M., Grogin N., Kocevski D., Koekemoer A., Somerville R. S., White C. E., 2014, *MNRAS*, 444, 2960
- Ellis R. S., McLure R. J., Dunlop J. S., Robertson B. E., Ono Y., Schenker M. A., Koekemoer A., Bowler R. A. A., Ouchi M., Rogers A. B., Curtis-Lake E., Schneider E., Charlot S., Stark D. P., Furlanetto S. R., Cirasuolo M., 2013, *ApJL*, 763, L7
- Erb D. K., Pettini M., Shapley A. E., Steidel C. C., Law D. R., Reddy N. A., 2010, *ApJ*, 719, 1168
- Ferland G. J., Porter R. L., van Hoof P. A. M., Williams R. J. R., Abel N. P., Lykins M. L., Shaw G., Henney W. J., Stancil P. C., 2013, *Rev. Mexicana Astron. Astrofis.*, 49, 137
- Finkelstein S. L., Papovich C., Salmon B., Finlator K., Dickinson M., Ferguson H. C., Giavalisco M., Koekemoer A. M., Reddy N. A., Bassett R., Conselice C. J., Dunlop J. S., Faber S. M., Grogin N. A., Hathi N. P., Kocevski D. D., Lai K., Lee K.-S., McLure R. J., Mobasher B., Newman J. A., 2012, *ApJ*, 756, 164
- Garnett D. R., Shields G. A., Peimbert M., Torres-Peimbert S., Skillman E. D., Dufour R. J., Terlevich E., Terlevich R. J., 1999, *ApJ*, 513, 168
- Garnett D. R., Skillman E. D., Dufour R. J., Peimbert M., Torres-Peimbert S., Terlevich R., Terlevich E., Shields G. A., 1995, *ApJ*, 443, 64
- Garnett D. R., Skillman E. D., Dufour R. J., Shields G. A., 1997, *ApJ*, 481, 174
- González V., Bouwens R., Illingworth G., Labbé I., Oesch P., Franx M., Magee D., 2014, *ApJ*, 781, 34
- Grazian A., Fontana A., Santini P., Dunlop J. S., Ferguson H. C., Castellano M., Amorin R., Ashby M. L. N., Barro G., Behroozi P., Boutsia K., Caputi K. I., Chary R. R., Dekel A., Dickinson M. E., Faber S. M., Fazio G. G., Finkelstein S. L., Galametz A., Giallongo E., Giavalisco M., Grogin N. A., Guo Y., Kocevski D., Koekemoer A. M., Koo D. C., Lee K.-S., Lu Y., Merlin E., Mobasher B., Nonino M., Papovich C., Paris D., Pentericci L., Reddy N., Renzini A., Salmon B., Salvato M., Sommariva V., Song M., Vanzella E., 2015, *A&A*, 575, A96
- Hainline K. N., Shapley A. E., Greene J. E., Steidel C. C., 2011, *ApJ*, 733, 31
- Hainline K. N., Shapley A. E., Kornei K. A., Pettini M., Buckley-Geer E., Allam S. S., Tucker D. L., 2009, *ApJ*, 701, 52
- Hashimoto T., Ouchi M., Shimasaku K., Ono Y., Nakajima K., Rauch M., Lee J., Okamura S., 2013, *ApJ*, 765, 70
- James B. L., Pettini M., Christensen L., Auger M. W., Becker G. D., King L. J., Quider A. M., Shapley A. E., Steidel C. C., 2014, *MNRAS*, 440, 1794
- Labbé I., Oesch P. A., Bouwens R. J., Illingworth G. D., Magee D., González V., Carollo C. M., Franx M., Trenti M., van Dokkum P. G., Stiavelli M., 2013, *ApJL*, 777, L19
- McLean I. S., Steidel C. C., Epps H. W., Konidaris N., Matthews K. Y., Adkins S., Aliado T., Brims G., Canfield J. M., Cromer J. L., Fucik J., Kulas K., Mace G., Magnone K., Rodriguez H., Rudie G., Trainor R., Wang E., Weber B., Weiss J., 2012, in *Society of Photo-Optical Instrumentation Engineers (SPIE) Conference Series*, Vol. 8446, Society of Photo-Optical Instrumentation Engineers (SPIE) Conference Series
- McLinden E. M., Finkelstein S. L., Rhoads J. E., Malhotra S., Hibon P., Richardson M. L. A., Cresci G., Quirrenbach A., Pasquali A., Bian F., Fan X., Woodward C. E., 2011, *ApJ*, 730, 136
- McLure R. J., Dunlop J. S., Bowler R. A. A., Curtis-Lake E., Schenker M., Ellis R. S., Robertson B. E., Koekemoer A. M., Rogers A. B., Ono Y., Ouchi M., Charlot S., Wild V., Stark D. P., Furlanetto S. R., Cirasuolo M., Targett T. A., 2013, *MNRAS*, 432, 2696
- Mesinger A., Aykotalp A., Vanzella E., Pentericci L., Ferrara A., Dijkstra M., 2015, *MNRAS*, 446, 566
- Oesch P. A., Bouwens R. J., Carollo C. M., Illingworth G. D., Trenti M., Stiavelli M., Magee D., Labbé I., Franx M., 2010, *ApJL*, 709, L21
- Oesch P. A., Bouwens R. J., Illingworth G. D., Labbé I., Smit R., Franx M., van Dokkum P. G., Momcheva I., Ashby M. L. N., Fazio G. G., Huang J.-S., Willner S. P., Gonzalez V., Magee D., Trenti M., Brammer G. B., Skelton R. E., Spitler L. R., 2014, *ApJ*, 786, 108
- Oke J. B., Gunn J. E., 1983, *ApJ*, 266, 713
- Ono Y., Ouchi M., Curtis-Lake E., Schenker M. A., Ellis R. S., McLure R. J., Dunlop J. S., Robertson B. E., Koekemoer A. M.,

- Bowler R. A. A., Rogers A. B., Schneider E., Charlot S., Stark D. P., Shimasaku K., Furlanetto S. R., Cirasuolo M., 2013, *ApJ*, 777, 155
- Pacifici C., Charlot S., Blaizot J., Brinchmann J., 2012, *MNRAS*, 421, 2002
- Richard J., Pei L., Limousin M., Jullo E., Kneib J. P., 2009, *A&A*, 498, 37
- Robertson B. E., Ellis R. S., Furlanetto S. R., Dunlop J. S., 2015, *ApJL*, 802, L19
- Robertson B. E., Furlanetto S. R., Schneider E., Charlot S., Ellis R. S., Stark D. P., McLure R. J., Dunlop J. S., Koekemoer A., Schenker M. A., Ouchi M., Ono Y., Curtis-Lake E., Rogers A. B., Bowler R. A. A., Cirasuolo M., 2013, *ApJ*, 768, 71
- Rogers A. B., McLure R. J., Dunlop J. S., 2013, *MNRAS*, 429, 2456
- Salmon B., Papovich C., Finkelstein S. L., Tilvi V., Finlator K., Behroozi P., Dahlen T., Davé R., Dekel A., Dickinson M., Ferguson H. C., Giavalisco M., Long J., Lu Y., Mobasher B., Reddy N., Somerville R. S., Wechsler R. H., 2015, *ApJ*, 799, 183
- Schenker M. A., Ellis R. S., Konidaris N. P., Stark D. P., 2013a, *ApJ*, 777, 67
- , 2014, *ApJ*, 795, 20
- Schenker M. A., Robertson B. E., Ellis R. S., Ono Y., McLure R. J., Dunlop J. S., Koekemoer A., Bowler R. A. A., Ouchi M., Curtis-Lake E., Rogers A. B., Schneider E., Charlot S., Stark D. P., Furlanetto S. R., Cirasuolo M., 2013b, *ApJ*, 768, 196
- Schenker M. A., Stark D. P., Ellis R. S., Robertson B. E., Dunlop J. S., McLure R. J., Kneib J.-P., Richard J., 2012, *ApJ*, 744, 179
- Shapley A. E., Steidel C. C., Pettini M., Adelberger K. L., 2003, *ApJ*, 588, 65
- Shim H., Chary R.-R., Dickinson M., Lin L., Spinrad H., Stern D., Yan C.-H., 2011, *ApJ*, 738, 69
- Smit R., Bouwens R. J., Franx M., Illingworth G. D., Labbé I., Oesch P. A., van Dokkum P. G., 2012, *ApJ*, 756, 14
- Smit R., Bouwens R. J., Franx M., Oesch P. A., Ashby M. L. N., Willner S. P., Labbé I., Holwerda B., Fazio G. G., Huang J.-S., 2015, *ApJ*, 801, 122
- Smit R., Bouwens R. J., Labbé I., Zheng W., Bradley L., Donahue M., Lemze D., Moustakas J., Umetsu K., Zitrin A., Coe D., Postman M., Gonzalez V., Bartelmann M., Benítez N., Broadhurst T., Ford H., Grillo C., Infante L., Jimenez-Teja Y., Jouvel S., Kelson D. D., Lahav O., Maoz D., Medezinski E., Melchior P., Meneghetti M., Merten J., Molino A., Moustakas L. A., Nonino M., Rosati P., Seitz S., 2014, *ApJ*, 784, 58
- Stark D. P., Ellis R. S., Ouchi M., 2011, *ApJL*, 728, L2
- Stark D. P., Richard J., Charlot S., Clement B., Ellis R., Siana B., Robertson B., Schenker M., Gutkin J., Wofford A., 2014a, Accepted in *MNRAS*, arxiv:1408.3649
- Stark D. P., Richard J., Siana B., Charlot S., Freeman W. R., Gutkin J., Wofford A., Robertson B., Amanullah R., Watson D., Milvang-Jensen B., 2014b, *MNRAS*, 445, 3200
- Stark D. P., Schenker M. A., Ellis R., Robertson B., McLure R., Dunlop J., 2013, *ApJ*, 763, 129
- Steidel C. C., Erb D. K., Shapley A. E., Pettini M., Reddy N., Bogosavljević M., Rudie G. C., Rakic O., 2010, *ApJ*, 717, 289
- Steidel C. C., Hunt M. P., Shapley A. E., Adelberger K. L., Pettini M., Dickinson M., Giavalisco M., 2002, *ApJ*, 576, 653
- Steidel C. C., Rudie G. C., Strom A. L., Pettini M., Reddy N. A., Shapley A. E., Trainor R. F., Erb D. K., Turner M. L., Konidaris N. P., Kulas K. R., Mace G., Matthews K., McLean I. S., 2014, *ApJ*, 795, 165
- Tapken C., Appenzeller I., Noll S., Richling S., Heidt J., Meinköhn E., Mehlert D., 2007, *A&A*, 467, 63
- Tilvi V., Papovich C., Finkelstein S. L., Long J., Song M., Dickinson M., Ferguson H. C., Koekemoer A. M., Giavalisco M., Mobasher B., 2014, *ApJ*, 794, 5
- Treu T., Schmidt K. B., Trenti M., Bradley L. D., Stiavelli M., 2013, *ApJL*, 775, L29
- Wilkins S. M., Bunker A. J., Stanway E., Lorenzoni S., Caruana J., 2011, *MNRAS*, 417, 717
- Zheng W., Postman M., Zitrin A., Moustakas J., Shu X., Jouvel S., Høst O., Molino A., Bradley L., Coe D., Moustakas L. A., Carrasco M., Ford H., Benítez N., Lauer T. R., Seitz S., Bouwens R., Koekemoer A., Medezinski E., Bartelmann M., Broadhurst T., Donahue M., Grillo C., Infante L., Jha S. W., Kelson D. D., Lahav O., Lemze D., Melchior P., Meneghetti M., Merten J., Nonino M., Ogaz S., Rosati P., Umetsu K., van der Wel A., 2012, *Nature*, 489, 406
- Zitrin A., Zheng W., Broadhurst T., Moustakas J., Lam D., Shu X., Huang X., Diego J. M., Ford H., Lim J., Bauer F. E., Infante L., Kelson D. D., Molino A., 2014, *ApJL*, 793, L12